Unpublished Report

Document ID:	SheepCRC_11_4
Title:	Diameter correction for clean colour measurement of wool
Author:	Wang, H.; Mahar, T.
Key words:	wool; colour measurement; diameter

This report was prepared as part of the Sheep CRC Program 2007-2014. It is not a refereed publication. If the report is quoted it should be cited as:

Sheep CRC Report 11_4

MODELLING OF DIAMETER-SCATTER TO DETERMINE A DIAMETER CORRECTION FOR CLEAN COLOUR MEASUREMENT OF MIDSIDE SAMPLES

CRC SII Project 2.2

August, 2009

Henry Wang and Trevor Mahar
AWTA LTD, PO Box 190, Guildford, NSW, 2161

Table of Contents

1 Background

Statistical analyses on colour testing data for raw wool have shown that yellowness (Y-Z) of clean wool is significantly correlated with Mean Fibre Diameter (MFD) (Mahar, 2007, Wang and Mahar, 2008, Fleet et al., 2009). As the current Sheep CRC Ltd project 2.2 is to provide Australian sheep breeders with the information required to improve the whiteness of Australian wool by genetic means, it should be beneficial to eliminate the effect of fibre diameter scatter from the colour test results. In this report, mathematical models are developed to determine a diameter-scatter correction for measurement of the clean colour of midside samples made using the AWTA Ltd Fleece Measurement 'standard'. This measurement is adapted from the International Wool Textile Organisation standard pre-sale colour test of raw wool - IWTO-56-07 (IWTO, 2007).

2 Complexity of colour measurement of wool

In general, when light passes through a medium and strikes an object which has a different refractive index from the medium, the interaction between the light and the material may involve reflection (I_r), transmission (I_t) and / or absorption (I_a). In particular, when the object is a particulate material, scattering (I_s) will occur instead of reflection. The scattering coefficient strongly depends on the ratio of the refractive indices of the particle and the surrounding medium, the number of particles (scattering centres) present, the ratio of the particle size to the wavelength of the light, and the particle shape (Tilley, 2000).

The appearance of a solid material is often dominated by reflection (I_r), which includes specular reflection and diffuse reflection. The proportion of the diffuse to specular reflections largely depends on the roughness of the material surface (Figure 1). With an increase of the surface roughness, the diffuse reflection increases, while specular reflection reduces.

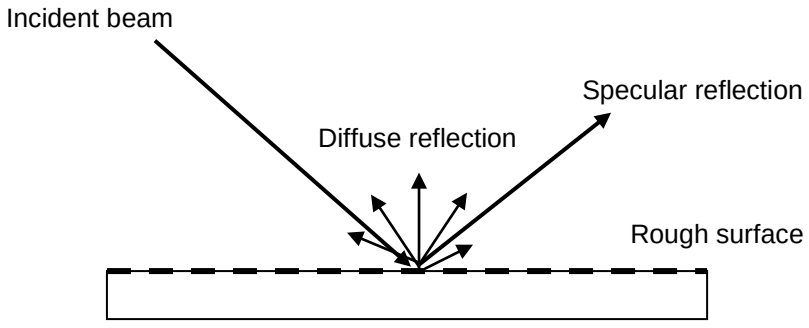

Figure 1. Light components in a surface reflectance

Wool is a translucent rather than a transparent or an opaque material. As Figure 2 shows, when a light beam strikes a wool fibre surface, some of the light is reflected from the surface (primary reflection), and some passes into the wool. Some light is internally reflected within the fibre and re-emerges with some wavelengths having been absorbed by chromophores present in the fibre medium (secondary reflection). Fibres

of higher diameter will absorb a higher amount of light than those of low diameter since by the Beer Lambert Law

$$A=e_{\lambda}cl \quad (1)$$

where e_{λ} is the molar absorption coefficient of the material at wavelength λ , c is concentration of absorbing materials and l is path length.

The transmitted light may be reflected from the surface of a second fibre and this multiple absorption / reflection process can occur up to the maximum depth of penetration of light into the bulk material which for wool is dependent on the density of the sample. Thus, the reflected light from a wool mat or fabric surface will consist of primary and multiply-reflected components.

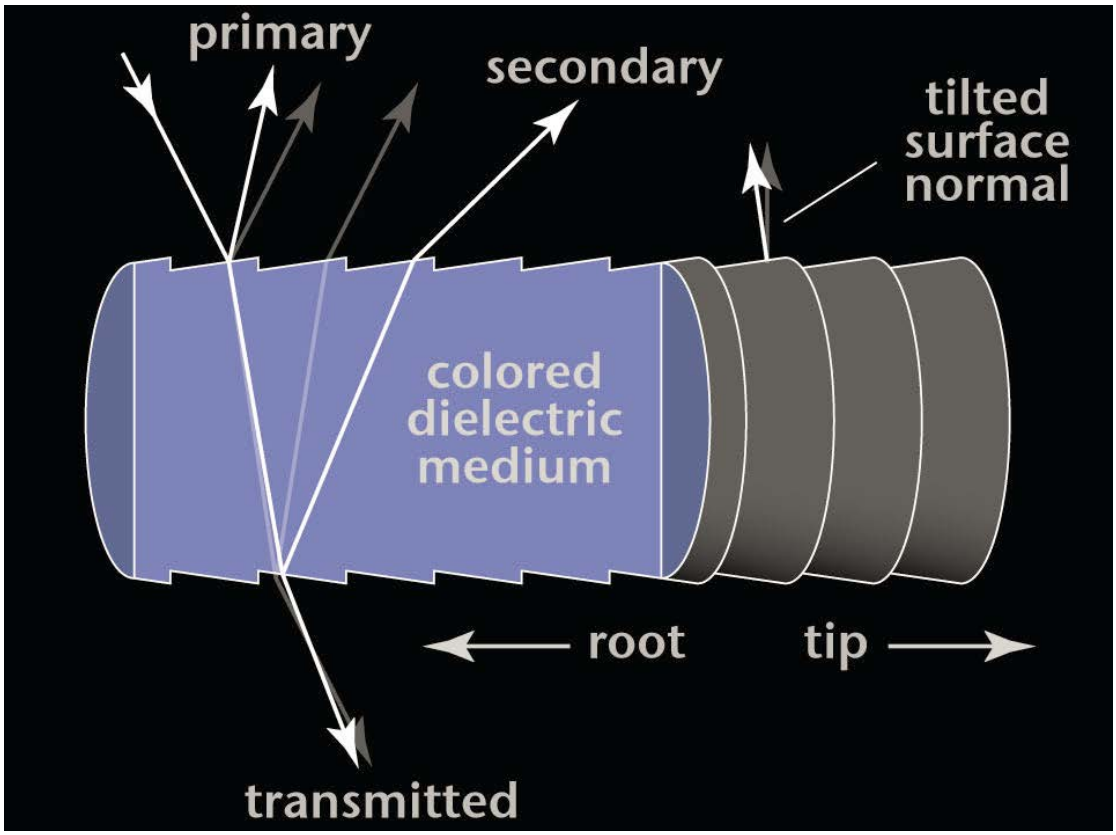

Figure 2. Light components in a light beam striking a wool fibre

In colour measurement of fibrous materials, the surface conditions and packing density of the fibres will affect the light distribution of specular and diffuse reflections. To measure the colour of clean wool based on IWTO-56, a $45^{o}/0^{o}$ or $0^{o}/45^{o}$ geometrical colour space (Figure 3) is configured to exclude the specular reflection from the wool bulk, which is pressed behind a glass. Diffuse reflection is therefore the major component involved in the measurement.

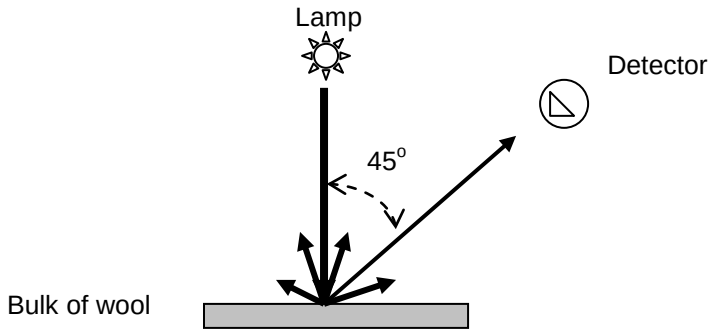

Figure 3. Colour instrument configuration of the $0^o/45^o$ geometrical space

A number of theories have been developed for approximating the phenomena of diffuse reflectance (Dahm and Dahm, 2007).

- The Stokes theory developed in the 1860s describes the reflection, absorption, and transmission through directly illuminated samples which are modelled as plane parallel layers.

- The Rayleigh theory developed late 1800s describes the scatter phenomenon of particles from which the particle size is much smaller than the wavelength of the light being scattered.

- The Mie theory developed in the early 1900s describes the absorption and scatter phenomena of spheres.

- The Schuster theory, also called two-flux theory, describes the scattering from a dilute suspension of particles, in which the distance between particles is large compared to the size of the particles. Each particle is assumed to scatter isotropically.

- The Kubelka - Munk theory (Kubelka and Munk, 1931) describes the remission and transmission of light through an infinitely thick sample. In particular, the Kubelka Munk theory details the properties of light scattering colorant layers and defines a relationship between spectral reflectance (R) of the sample and its absorption (K) and scattering (S) characteristics as follows:

-

$$(1-R_\infty)^2 / 2R_\infty = K/S \qquad (2)$$

Where R_∞ is the spectral reflectance from an infinite thickness of a sample.

For textile materials, it is assumed that the scattering (S) of a dye or pigment depends on the properties of the substrate or opacifier, while the absorption (K) of light depends on the properties of colorant.

3 Modelling of diameter-scatter correction on colour results

3.1 Techniques for separating physical scattering and chemical absorbance in diffusing reflectance spectra

Techniques are not currently available for diameter-scattering correction for colour (wavelengths: 400nm – 700nm) measurement, but there have been significant developments in the understanding of scattering in a similar electromagnetic radiation, Near Infra-Red (NIR, wavelengths: 800nm – 2500nm). With the development of process analytical technology (PAT), vibrational spectroscopy (i.e. NIR, infrared (IR) and Raman) has become a major non-destructive tool in many applications within the chemical, pharmaceutical, food and agricultural industries. In particular, NIR technology has evolved rapidly since the 1970s and is a well recognised substitute for a number of time-consuming analytical techniques. AWTA Ltd has well established NIR techniques in the prediction of the Residual Grease and the Ash content of raw wool.

Based on the sensitivity of NIR spectra to scattering, research has been reported, in which NIR spectral data were used to predict the Mean Fibre Diameter (MFD) of wool fibres. (Cozzolino et al., 2005, Hammersley and Townsend, 2008). If scattering can be used to quantify MFD of fibres using NIR it is reasonable to expect that corrections can be developed for diameter scattering in colour measurement.

In NIR prediction of the chemical constituents of materials, one task of signal processing is to separate the spectral components determined by the physical and chemical properties of the material, which are combined in the measured spectra. Techniques developed for this signal separation include standard normal variates (SNV), multiplicative signal correction (MSC) and extended multiplicative signal correction (EMSC) (Martens et al., 2003, Kessler et al., 2009). These methods have been used successfully to remove or eliminate the unwanted scatter information caused by morphological variations between samples. All are preprocessing techniques used to modify measured spectra prior to chemical analysis. MSC quantifies the effect on spectral response of physical variations in the measured material, such as variations in light scattering due to sample packaging, sample surface topography, particle size etc., in regions of the spectrum where there is no expected effect on response due to chemical variations in the material under test. EMSC is an extension of MSC which overcomes problems with systematic chemical variations and instances in which the physical and chemical effects are seriously entangled in the spectra. Further details of these techniques are beyond the scope of this report and can be obtained from the references provided.

The EMSC method was developed and improved by Stark and Martens (Stark and Martens, 1996, Stark and Martens, 1997). EMSC applies a scatter-correction to each measured spectrum according to the general equation:

$$R_i \approx a_i + b_i R_{i,chem.} + d_i\lambda + e_i\lambda^2 \quad (3)$$

Where:

a_i represents the baseline offset of the spectrum for the ith sample;

b_i represents the path length relative to a reference spectrum for the ith sample;

d_i and e_i stand for unknown wavelength (λ)-dependent spectral variations from sample to sample.

$R_{i,chem.}$ represents the spectrum resulting from the pure chemical properties of the ith sample.

Therefore, in the colour spectrum of the ith sample:

$$R_{i,colorant} \approx R_{i,corrected} = (R_i - a_i - d_i\lambda - e_i\lambda^2) / b_i \quad (4)$$

Estimates of the model parameters, a_i, b_i, d_i and e_i, can be obtained based on the measured R_i at the wavelengths which are insensitive to variations in the chemical constituents (Martens et al., 2003).

The EMSC pretreatment on the raw spectra can be readily performed by a commercial multivariate calibration programme, and the corresponding $R_{i,corrected}$ spectra can be obtained directly. The Unscrambler software (CAMO Inc., Norway) was used to perform the EMSC pretreatment in the present report.

3.2 Assumptions of the models

To model the diameter-scatter effect on colour results, the following aspects need to be considered:

- Variations in fibre diameter and colorants of samples;
- Variations in light scattering and absorption among samples;
- Uniformity of sample packing density presented to the colorimeter; and,
- Presentation of samples to the colorimeter.

The following assumptions apply to the model under discussion:

- Fibre diameter-scatter is the dominant component and within fibre pigment-scatter is a relatively weak source of light scattering.
- At the same angle of incidence, the amount of light absorbed and scattered by individual wool fibres of similar diameter is a constant fraction of the intensity incident upon the fibres. This fraction is independent of where the fibres are located within the sample bulk;
- The variation of diameter along a fibre is ignored, there are no voids within individual fibres, and fluorescence is not considered;
- The thickness of a 5g pressed fibre bulk is infinite for the diffusing reflectance in the ‘standard’ colour test, and the packing density is uniform across the bulk volume; and,
- The refractive index is dispersionless, i.e., constant across the light wavelength range.

3.3 Methodology of modelling

The AWTA Fleece Measurement 'standard' reports the CIE tristimulus values. These X, Y, Z values are calculated from spectrophotometric data according to the following equations (Billmeyer and Saltzman, 1966).

$$X = \frac{100\int E_\lambda R_\lambda \bar{x}_\lambda d\lambda}{\int E_\lambda R_\lambda \bar{y}_\lambda d\lambda} \quad (5)$$

$$Y = \frac{100\int E_\lambda R_\lambda \bar{y}_\lambda d\lambda}{\int E_\lambda R_\lambda \bar{y}_\lambda d\lambda} \quad (6)$$

$$Z = \frac{100\int E_\lambda R_\lambda \bar{z}_\lambda d\lambda}{\int E_\lambda R_\lambda \bar{y}_\lambda d\lambda} \quad (7)$$

Where:

X, Y, and Z are the CIE tristimulus values;

λ is wavelength;

R_λ is the spectral reflectance of the sample;

E_λ is the relative spectral energy of the light source; and,

$\bar{x}_\lambda$, $\bar{y}_\lambda$ and $\bar{z}_\lambda$ are the tristimulus values of the spectrum colours.

In the calculations, only R_λ contains all spectral response of the sample being tested. This spectral information includes:

- the absorbance by the colorants ($R_{\lambda,col}$);
- the scattering ($R_{\lambda,scat}$) from the fibres due to the baseline offset and path length changes (related to fibre diameter and packing density etc).

Therefore,

$$R_\lambda = R_{\lambda,col} + R_{\lambda,scat} \quad (8)$$

$$R_{\lambda,col} = R_\lambda - R_{\lambda,scat} \quad (9)$$

As indicated earlier, the EMSC technique can remove $R_{\lambda,scat}$ from R_λ and generates a spectrum $R_{\lambda,EMSC}$ which is approximately equal to $R_{\lambda,col}$. Therefore, the difference $\Delta R_\lambda = R_\lambda - R_{\lambda,EMSC}$ will reflect the scattering effects of fibre diameter and be diameter dependent. That is, the relationship $\Delta R_\lambda \propto MFD$ is the focus of this model development.

In the first instance, a linear relationship is assumed:

$$\Delta R_\lambda = \alpha_\lambda * MFD + \beta_\lambda, \text{ therefore,} \quad (10)$$

$$
\begin{aligned}
X_{corrected} &= \frac{100\int E_\lambda R_{\lambda,col}\bar{x}_\lambda d\lambda}{\int E_\lambda R_\lambda \bar{y}_\lambda d\lambda} \\
&= \frac{100\int E_\lambda (R_\lambda - \Delta R_\lambda)\bar{x}_\lambda d\lambda}{\int E_\lambda R_\lambda \bar{y}_\lambda d\lambda} \\
&= \frac{100\int E_\lambda R_\lambda \bar{x}_\lambda d\lambda}{\int E_\lambda R_\lambda \bar{y}_\lambda d\lambda} - \frac{100\int E_\lambda \Delta R_\lambda \bar{x}_\lambda d\lambda}{\int E_\lambda R_\lambda \bar{y}_\lambda d\lambda} \\
&= X_{raw} - \frac{100\int E_\lambda (\alpha_\lambda * MFD + \beta_\lambda)\bar{x}_\lambda d\lambda}{\int E_\lambda R_\lambda \bar{y}_\lambda d\lambda} \\
&= X_{raw} - \left(\frac{100\int E_\lambda (\alpha_\lambda * MFD)\bar{x}_\lambda d\lambda}{\int E_\lambda R_\lambda \bar{y}_\lambda d\lambda} + \frac{100\int E_\lambda \beta_\lambda \bar{x}_\lambda d\lambda}{\int E_\lambda R_\lambda \bar{y}_\lambda d\lambda}\right) \\
&= X_{raw} - \left(\frac{100\int E_\lambda \alpha_\lambda \bar{x}_\lambda d\lambda}{\int E_\lambda R_\lambda \bar{y}_\lambda d\lambda} * MFD + \frac{100\int E_\lambda \beta_\lambda \bar{x}_\lambda d\lambda}{\int E_\lambda R_\lambda \bar{y}_\lambda d\lambda}\right)
\end{aligned} \tag{11}
$$

Let $a_x = \frac{100\int E_\lambda \alpha_\lambda \bar{x}_\lambda d\lambda}{\int E_\lambda R_\lambda \bar{y}_\lambda d\lambda}$, and, (12)

$b_x = \frac{100\int E_\lambda \beta_\lambda \bar{x}_\lambda d\lambda}{\int E_\lambda R_\lambda \bar{y}_\lambda d\lambda}$, then, (13)

$$X_{corrected} = X_{raw} - (a_X * MFD + b_X) \tag{14}$$

The same derivation applies to Y, Z and (Y-Z):

$$Y_{corrected} = Y_{raw} - (a_Y * MFD + b_Y) \tag{15}$$

$$Z_{corrected} = Z_{raw} - (a_Z * MFD + b_Z) \tag{16}$$

$$(Y-Z)_{corrected} = (Y-Z)_{raw} - [(a_Y - a_Z) * MFD + (b_Y - b_Z)] \tag{17}$$

3.4 Experimental

In theory, the EMSC technique can treat any spectra which contains multiplicative signals (Martens et al., 2003, Kessler et al., 2009). However, in order to examine the feasibility of this theory for the current colour measurement, a well controlled extrusion trial was designed to produce a batch of polypropylene (PP) filaments which were chemically stable and contained no pigments. The resulting filaments had the same degree of crystallisation but different filament diameters. Thus, the effects of only fibre

diameter-scatter can be expected to be well presented in the reflectance spectra of these filaments. After the models were validated for the PP filaments, the model was then developed for wool midside samples using the same procedure. As the light scattering and absorbance are different between PP filaments and wool fibres, the models were different.

3.4.1 Polypropylene filaments

A single batch of PP filaments of eight (8) different MFD's was produced under the same conditions of viscosity at Deakin University. The extrusion parameters were as follows:

Raw Material	Polypropylene-Basell Moplen APD-258	
Extruder	Wayne Single Screw Desktop Extruder	
Die Used	18 Filaments	
Machine Settings		
	Temperature zone	Degree F
	Zone 1	330
	Zone 2	380
	Die Zone 1	390
	Die Zone 2	395
	Die Zone 3	402
	Screw Speed:	20 RPM

The same extrusion settings were used to ensure production of relatively homogeneous crystallisation of the eight (8) filaments. Subsequent differential scanning calorimetry (DSC) testing confirmed a consistent level of crystallisation formed in the PP filaments (Table 1). The controlled level of crystallisation would be expected to yield consistent internal light scattering within the resulting filaments. Therefore, the effect of the diameter on the light scattering can be isolated from the reflectance spectra.

The diameter characteristics of the PP filaments are listed in Table 2, which highlights MFD range of 11.3 μm (from 22.0μm – 33.3μm). Due to the limit of the winding speed on the extruder, finer diameters (16 μm – 20μm) were unachievable.

The set-up of the colorimeter is shown in Figure 4. The preparation of the PP filaments for the measurement was to cut the filaments into approximately 100mm lengths and then manually mix 5g of the resulting 'fibres' as uniformly as possible before presenting them to the colorimeter according to the 'standard' method. The spectra were obtained for each sample. The CIE X, Y, Z values are shown in Figure 5. The CIE X, Y, Z values decreased approximately linearly with an increase in fibre diameter.

Table 1. Crystallisation degree of the PP filaments from the DSC testing

LN	Cryst. point (^{o}C)	Peak point (^{o}C)	Heat (J/g)	Cryst. Degree (%)	SD of Cryst. (%)
43843.2	152.87	162.56	104.23	50.37	0.24
43844.3	153.52	161.96	102.40	49.47	1.23
43842.1	153.69	164.13	100.45	48.52	0.68
43840.6	153.35	163.74	97.40	47.05	0.52
43838.4	152.45	161.83	102.63	49.57	0.67
43839.5	152.35	163.50	101.78	49.17	1.09
43841	152.60	162.80	104.73	50.60	1.47
43846.5	152.70	162.68	107.80	52.07	1.80
Mean	152.94	162.90	102.68	49.60	0.96
SD	0.51	0.83	3.08	1.49	0.53

Note: Cryst. means crystallisation and SD, standard deviation

Table 2. Fibre diameter characteristics of eight PP filaments

LN	Winding speed (rpm)	MFD (μm)	SD (μm)	CV (%)
43843.2	312	22.0	3.2	14.3
43844.3	267	24.0	3.3	13.7
43842.1	250	24.5	3.3	13.6
43840.6	210	26.1	3.5	13.3
43838.4	192	27.0	3.9	14.3
43839.5	161	29.5	4.2	14.1
43841.0	145	31.0	4.1	13.2
43846.5	132	32.8	5.5	16.7

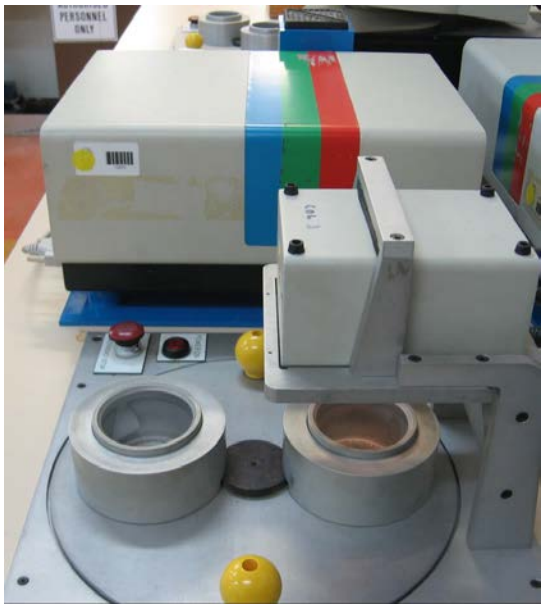

(a) Colorimeter

(b) Sample presentation

Figure 4. Standard colour measurement system at AWTA Ltd

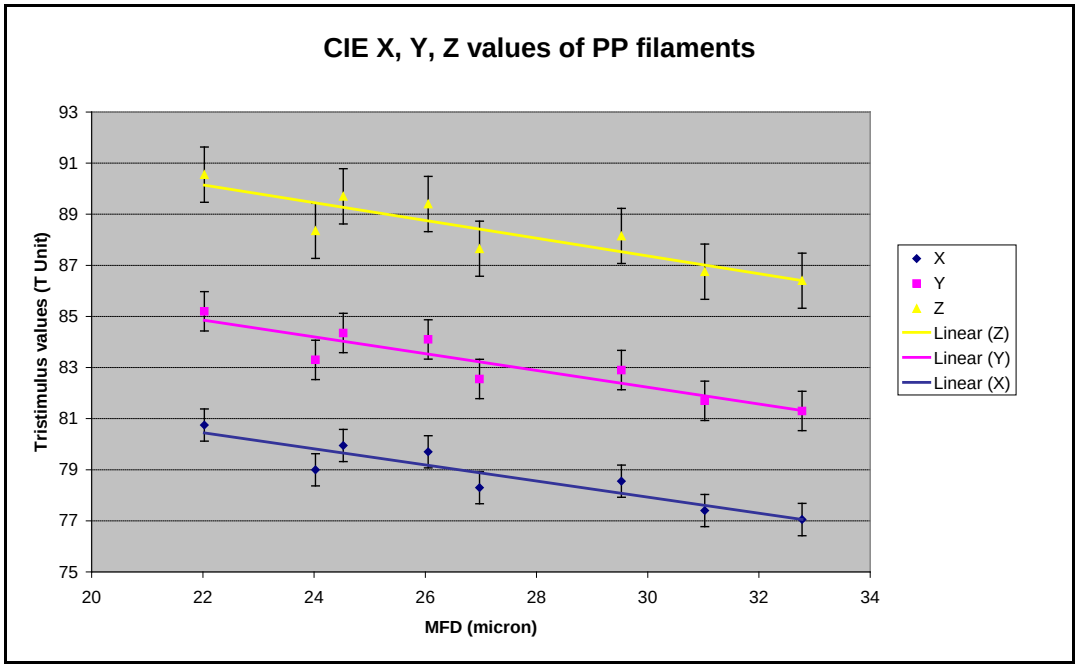

Figure 5. CIE X, Y, Z values of PP filaments from the 'standard' testing.

3.4.2 Colour measurement of midside samples

As midside samples from the same Information Nucleus Flock (INF) might provide wool samples with the least variation in colorants for a range of MFD values, ten (10) midside samples were selected from the Kirby INF. Their MFD's ranged from 13.5μm – 20.3μm. Colour measurement was carried out according to the 'standard' and results are listed in Table 3. In particular, the Y-Z values increased linearly with an increase in

MFD, as reported in an earlier survey of covering the full range of MFD values in the Australian wool clip (Wang and Mahar, 2008).

Table 3. Colour values of ten (10) midside samples from the CRC Kirby INF

LN	MFD (μm)	X	Y	Z	Y-Z
61225.3	13.5	71.2	75.4	68.8	6.6
61067.6	13.6	72.2	76.5	69.8	6.8
61032.6	14.1	71.8	76.6	69.4	7.2
61001.3	15.1	71.7	75.9	68.7	7.2
61224.2	16.1	70.1	74.2	66.7	7.5
61194.0	17.1	71.5	75.8	68.3	7.5
61129.5	18.1	71.0	75.3	67.5	7.8
61193.6	19.0	72.3	76.7	68.7	8.0
61003.5	19.5	71.1	75.4	67.4	8.0
61037.4	20.3	70.9	75.1	67.2	7.9

3.5 Development of the diameter correction models

From the colour testing, the R_λ spectra in the visible range (380nm – 720nm) were extracted at 10nm intervals for each sample. Then, the spectra were pretreated by the EMSC method in The Unscrambler software and the spectra $R_{\lambda,EMSC}$ were derived. The measured (R_λ) and treated ($R_{\lambda,EMSC}$) spectra are shown in Figures 6 to 9 for both the PP filaments and the midside samples, respectively.

Figure 6 clearly shows that the fibre diameter had a significant effect on the spectral intensity of the PP filaments. The coarser the fibres are, the less diffusing reflectance there is. After the EMSC pretreatment, the diameter effect was successfully removed from the R_λ of the PP filaments as shown in Figure 7.

Figure 8 shows the spectra of the 10 midside samples. Unlike the smoothed surface, clear PP filaments, wool fibres have scales covering the surface and internal colorants. The light scattering behaviour of the wool sample is therefore very different from the PP filaments even though their MFD values are similar. This is because both diameter–scatter and colorant-absorption combine to influence the measured spectra during a colour test. However, the EMSC method was still able to remove the diameter-scatter effect from the spectra as shown in Figure 9.

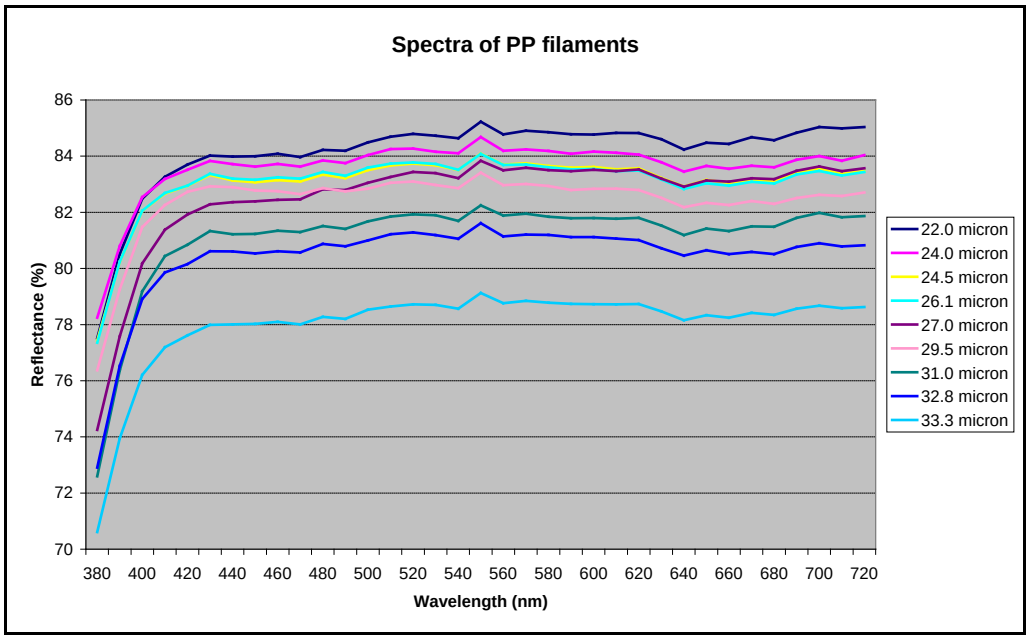

Figure 6. Colour spectra of PP filaments

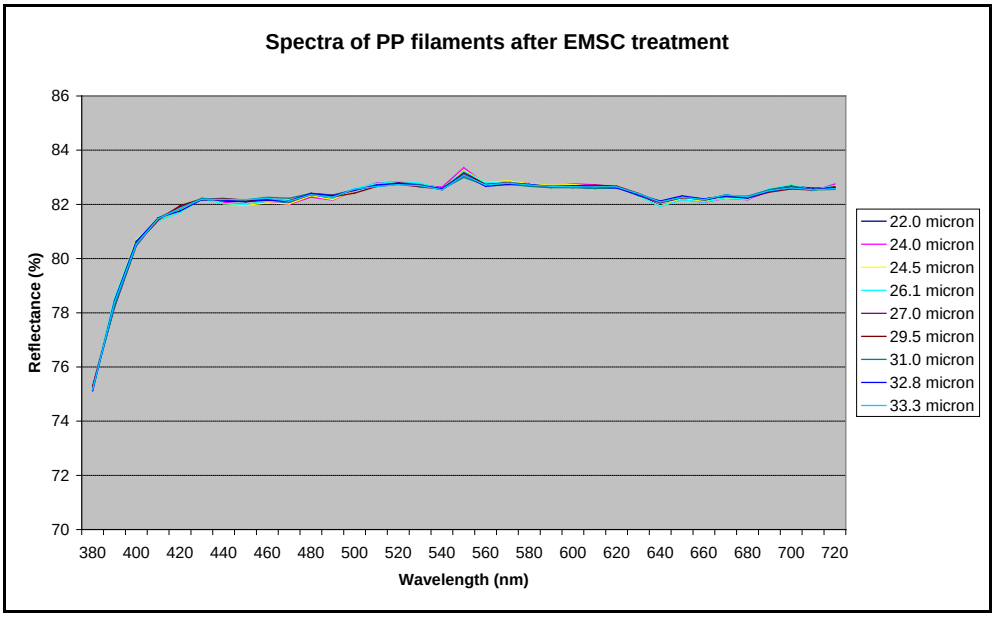

Figure 7. Colour spectra of PP filaments after EMSC treatment

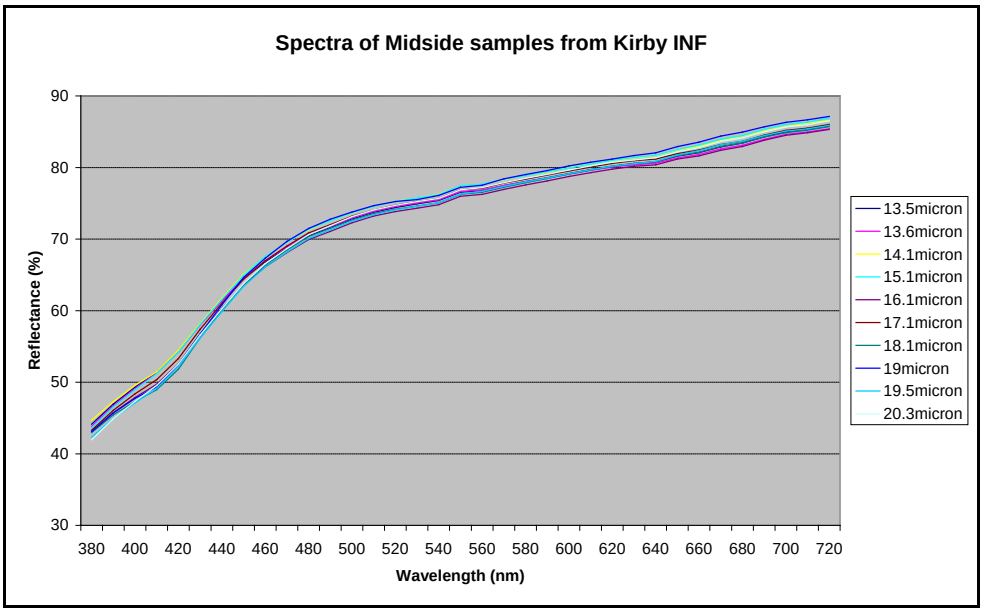

Figure 8. Colour spectra of midside samples

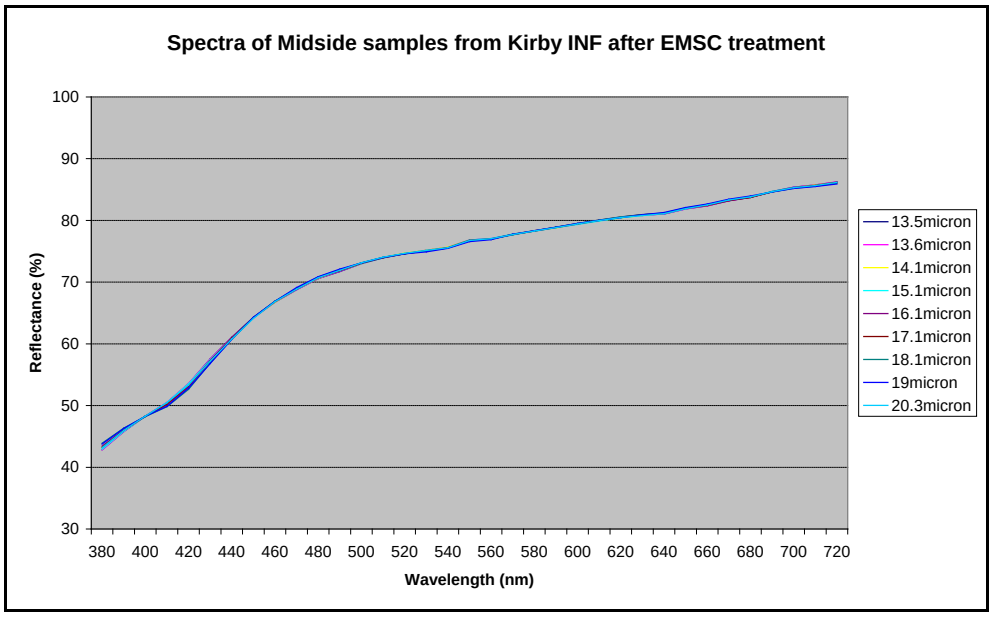

Figure 9. Colour spectra of midside samples after EMSC treatment

3.5.1 PP filaments

Based on the R_λ and $R_{\lambda,EMSC}$ spectra, linear relationships between the ΔR_λ (R_λ - $R_{\lambda,EMSC}$) and MFD were firstly derived wavelength by wavelength. Then the correction models were derived using equations (12) & (13).

For the PP filaments, the models for correcting the CIE X, Y, Z values are shown in Table 4.

Table 4. Models for PP filaments

Model	X	Y	Z
a	-0.295	-0.306	-0.329
b	8.477	8.793	9.504

The diameter corrections for X, Y, Z values are show in Figure 10. Analyses of variance (ANOVA) of the linear regressions are shown in Table 5. Comparison of the regressions before and after the corrections shows that the diameter dependence of the tristimulus values was successfully removed by the models. The regression relationships between the CIE X, Y, Z values and MFD became insignificant after application of the corrections. The reduction of the regression slopes is highly significant (Table 6).

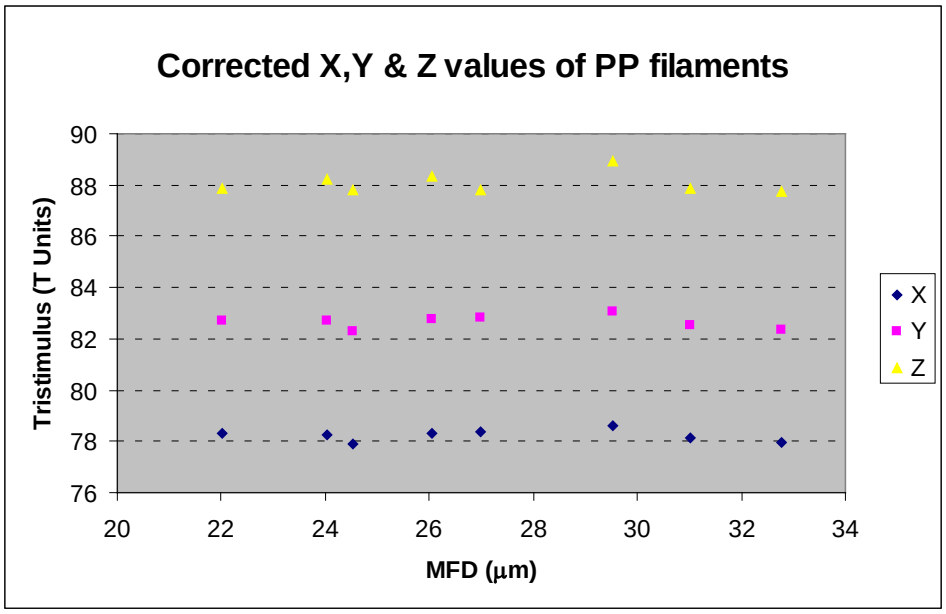

Figure 10. The relationships between corrected CIE X, Y, Z values and MFD of the PP filaments

Table 5. ANOVA of the linear regressions between X, Y, Z values and MFD for PP filaments

Tristimulus	Correction	*component*	*df*	*SS*	*MS*	*F*	*Significance F*
X	Before	Regression	1	8.851	8.851	137.893	0.000
		Residual	6	0.385	0.064		
		Total	7	9.236			
	After	Regression	1	0.006	0.006	0.095	0.769
		Residual	6	0.385	0.064		
		Total	7	0.391			
Y	Before	Regression	1	9.706	9.706	138.983	0.000
		Residual	6	0.419	0.070		
		Total	7	10.125			
	After	Regression	1	0.012	0.012	0.174	0.691
		Residual	6	0.419	0.070		
		Total	7	0.431			
Z	Before	Regression	1	10.138	10.138	51.604	0.000
		Residual	6	1.179	0.196		
		Total	7	11.317			
	After	Regression	1	0.002	0.002	0.011	0.919
		Residual	6	1.179	0.196		
		Total	7	1.181			

Table 6. Slope changes of the regressions between X, Y, Z values and MFD for PP filaments

Tristimulus	Model correction	
	Before	After
X	-0.303	-0.008
Y	-0.317	-0.011
Z	-0.324	0.005

3.5.2 Wool

Using the same methods as for the PP filaments, the models developed for the wool midside samples of the Kirby INF are listed in Table 7. As expected, these models have different slope and offset values compared to the PP models. A further difference is that, unlike the PP corrections in which the slopes and offset values were similar for X, Y and Z, the slope and offset of the wool model for Z were quite different from the X and Y values. This difference is mainly due to the absorption of UV and blue wavelengths by yellow chromophores present in the wool fibres. Figures 6 and 8 confirm the relatively constant reflectance across the visible wavelength band for the PP filaments (Figure 6) compared to wool (Figure 8) which shows a distinctly increased slope below 470nm. This higher slope coincides with the wavelength region which largely determines the Z values and has negligible effect on the X and Y values (Billmeyer and Saltzman, 1966). As a result, the ‘blue’ light range (Z) which includes the lowest visible wavelengths had higher spectral variation than the ‘yellow’ (Y) and ‘red’ (X) wavelength ranges.

Table 7. Models for midside samples

Model	**X**	**Y**	**Z**
a	-0.021	-0.014	-0.158
b	0.344	0.237	2.622

For the interests of the CRC project, the performance of the models is shown in Figures 11 &12 for Y-Z and Y values. The ANOVA of the linear regressions between the Y-Z and Y values and MFD are listed in Tables 8 & 9. The diameter dependence of Y-Z values was successfully removed after the model corrections. The regression relationships became insignificant (Table 8) and the regression slopes approached zero (Table 9).

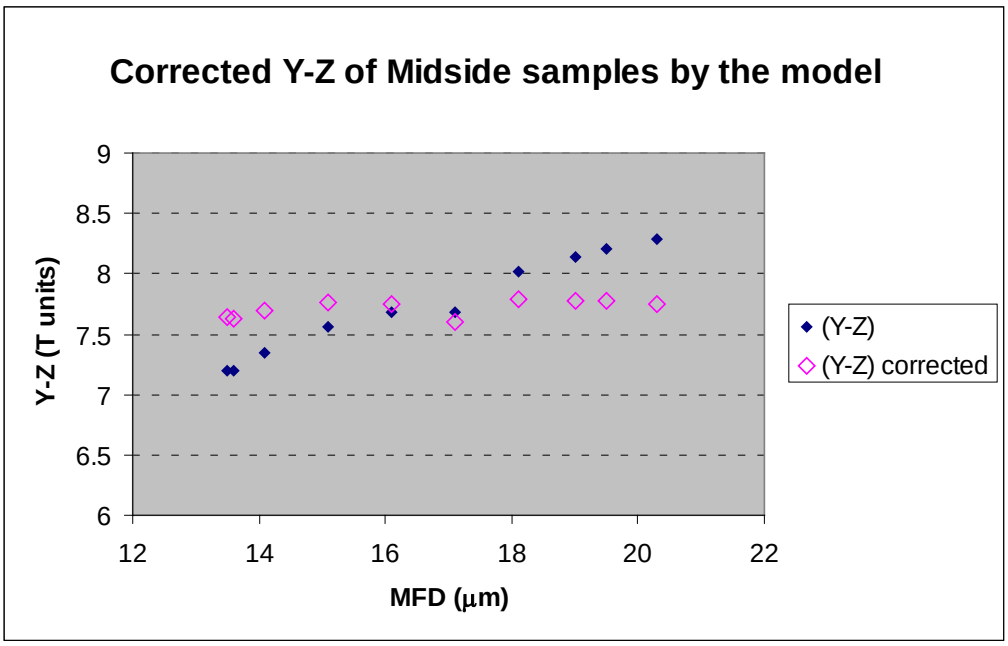

Figure 11. Performance of the model for (Y-Z) values of midside samples

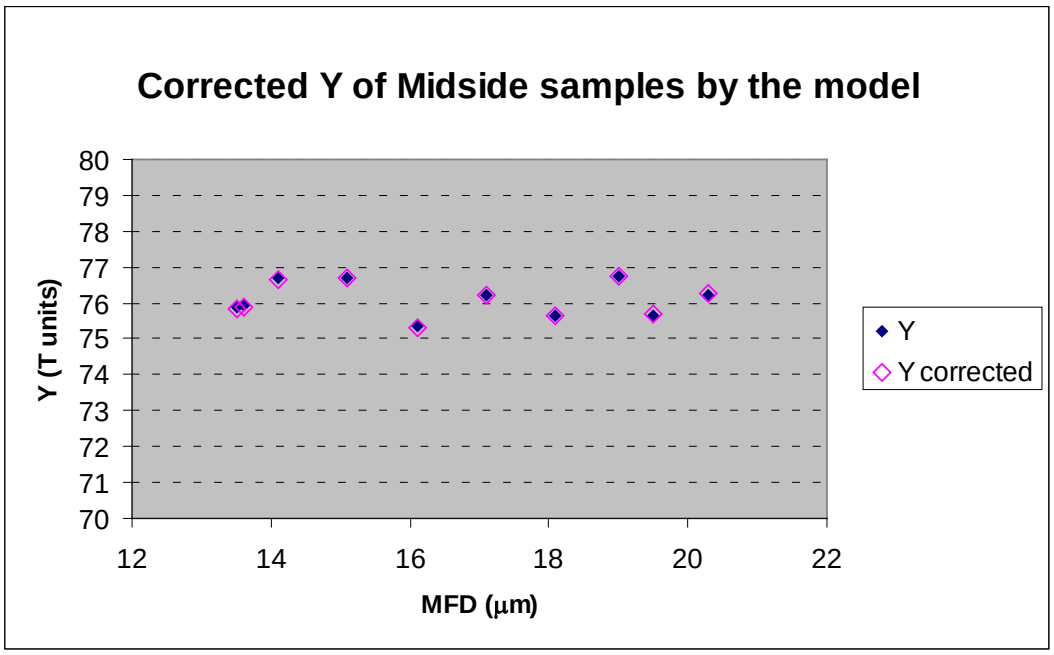

Figure 12. Performance of the model for Y values of midside samples

Table 8. ANOVA of the linear regressions between X, Y, Z values and MFD for midside samples

Colour	Correction	*Component*	*df*	*SS*	*MS*	*F*	*Significance F*
Y-Z	Before	Regression	1	1.501	1.501	410.965	0.000
		Residual	8	0.029	0.004		
		Total	9	1.530			
	After	Regression	1	0.017	0.017	4.708	0.062
		Residual	8	0.029	0.004		
		Total	9	0.046			
Y	Before	Regression	1	0.014	0.014	0.049	0.830
		Residual	8	2.186	0.273		
		Total	9	2.199			
	After	Regression	1	0.000	0.000	0.000	0.985
		Residual	8	2.186	0.273		
		Total	9	2.186			

Table 9. Slope changes of the regressions between Y-Z & Y values and MFD for midside samples

Colour	Model correction	
	Before	After
Y-Z	0.161	0.017
Y	-0.015	-0.001

3.6 Validation of the correction models

Validation of the models for the clean colour of midside samples was performed for all the INF's which were tested by the AWTA Sydney laboratory for Sheep CRC Ltd in the 2008 -2009 season. The performance of the models for both Y-Z and Y is shown in Figures 13-19 for each of the INF's. The diameter dependence of the (Y-Z) values caused by the diameter-scatter was either eliminated or significantly reduced by the models for each of the INF's. In particular, the correlation coefficients between MFD and (Y-Z) values were each reduced significantly by the corrections (Table 10). The regression slopes also were greatly reduced in absolute value in each case (Table 11). Consequently, the validations were considered successful for all flocks.

It is interesting to further examine the colour characteristics of INF 05, for which a relatively strong relationship between (Y-Z) and MFD remained after correction (Figure 16). It may be that the colorants of the wool samples are quite different across the MFD range for this flock. Visual examination of the MFD versus (Y-Z) plots shows that the model reduced the MFD dependence on measured (Y-Z) values for all data of this flock, but that a small number of the samples at the high diameter end appeared to exert high leverage on the regression slope. Removal of the three (3) samples with MFD > 17.5mm and (Y-Z) > 8.5 reduced the correlation coefficient and slope of the regression relationship to values consistent with the other flocks.

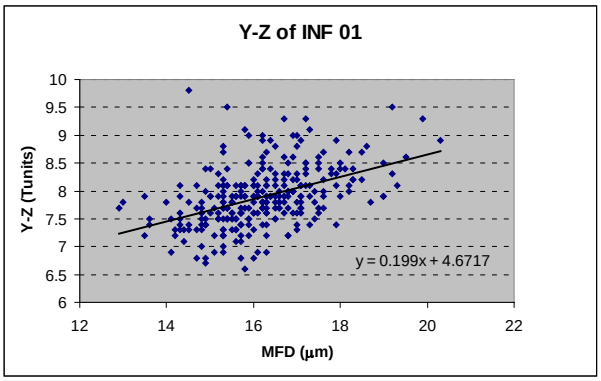

(a) Y-Z (before)

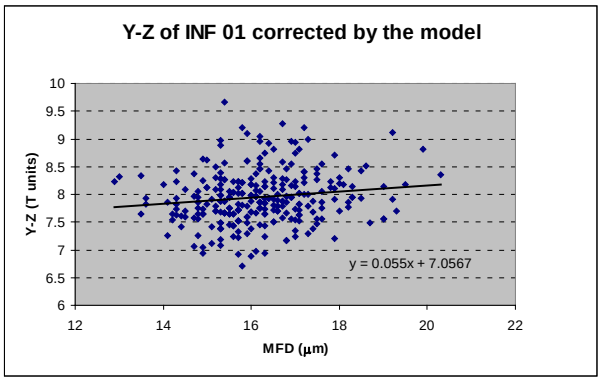

(b) Y-Z (after)

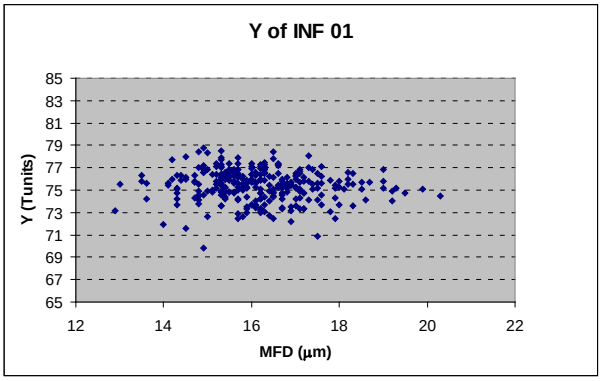

(c) Y (before)

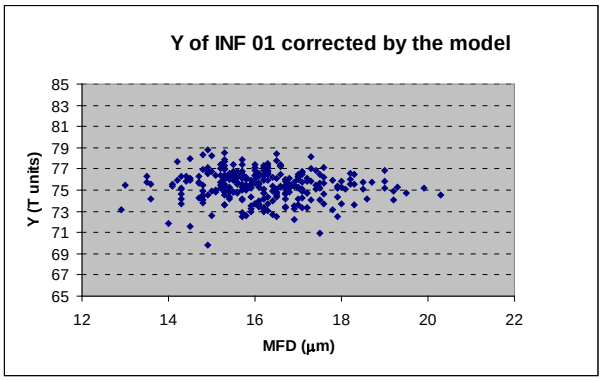

(d) Y (after)

Figure 13. Model performance for INF 01 (Kirby)

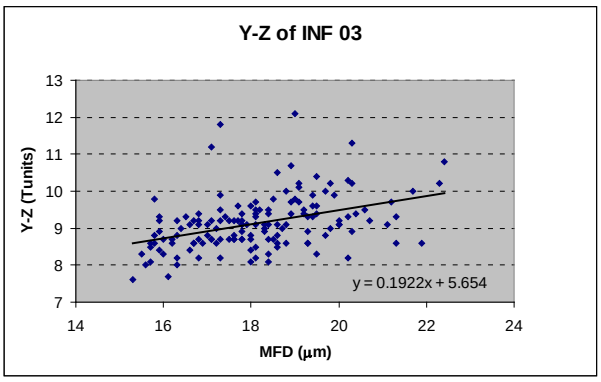

(a) Y-Z (before)

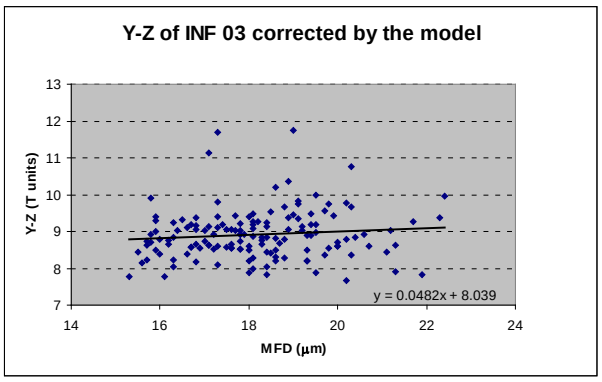

(b) Y-Z (after)

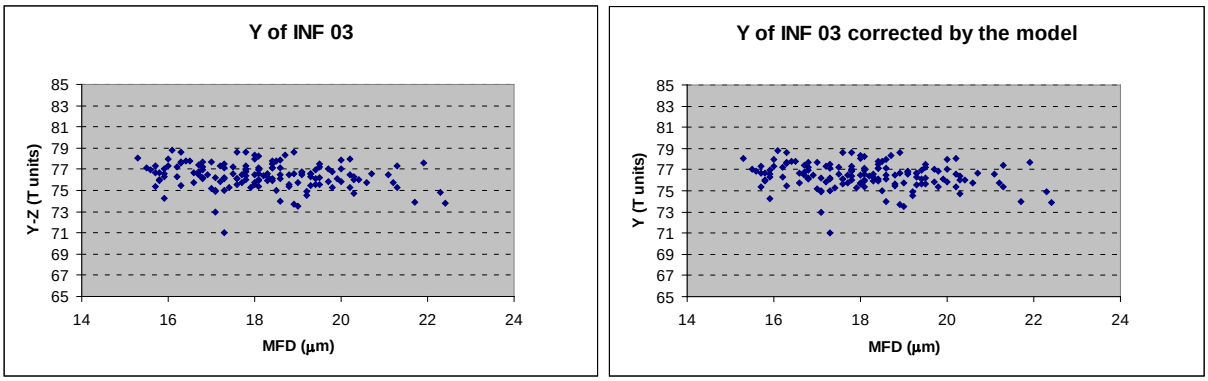

(c) Y (before) (d) Y (after)

Figure 14. Model performance for INF 03 (Cowra)

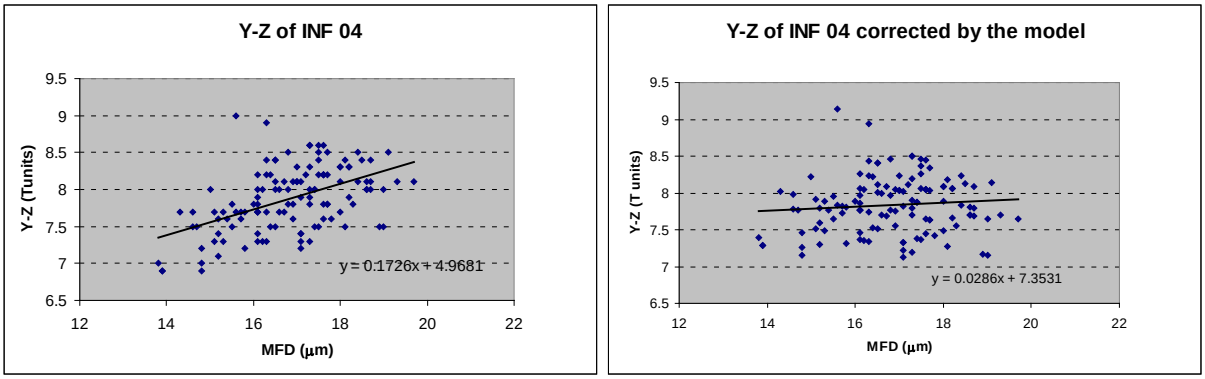

(a) Y-Z (before) (b) Y-Z (after)

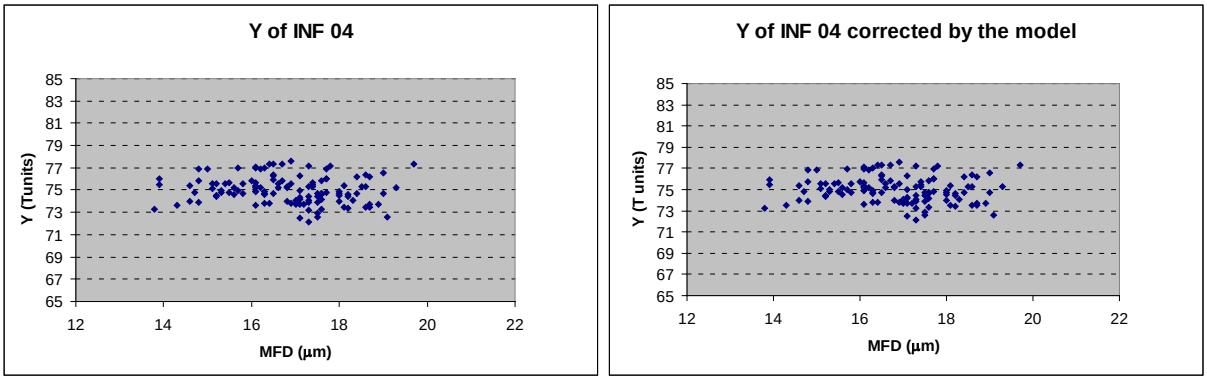

(c) Y (before) (d) Y (after)

Figure 15. Model performance for INF 04 (Rutherglen)

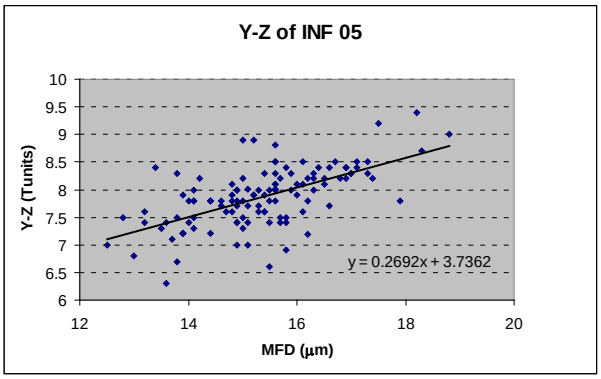

(a) Y-Z (before)

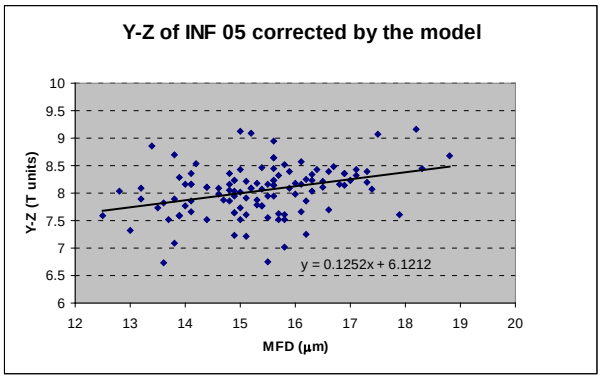

(b) Y-Z (after)

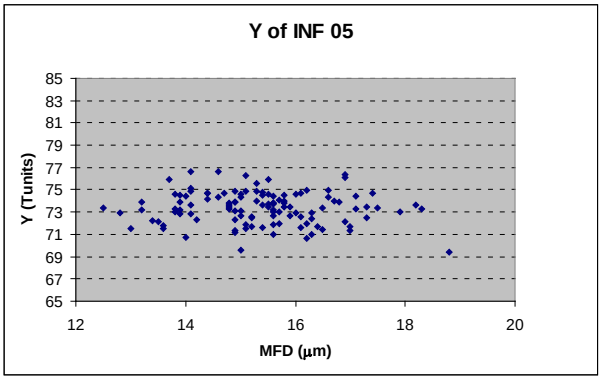

(c) Y (before)

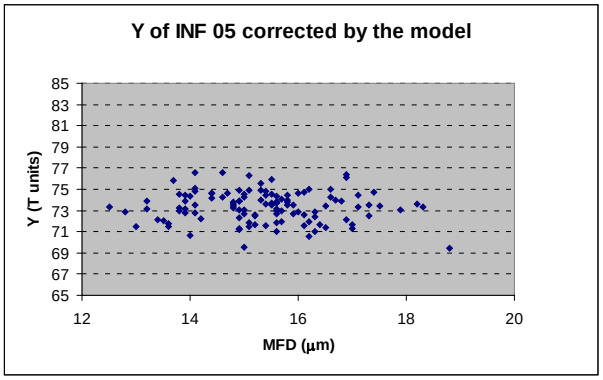

(d) Y (after)

Figure 16. Model performance for INF 05 (Hamilton)

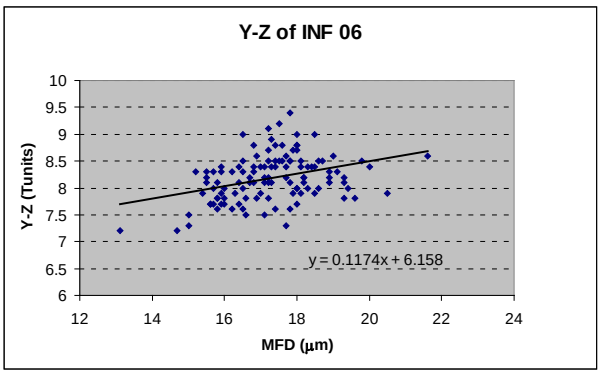

(a) Y-Z (before)

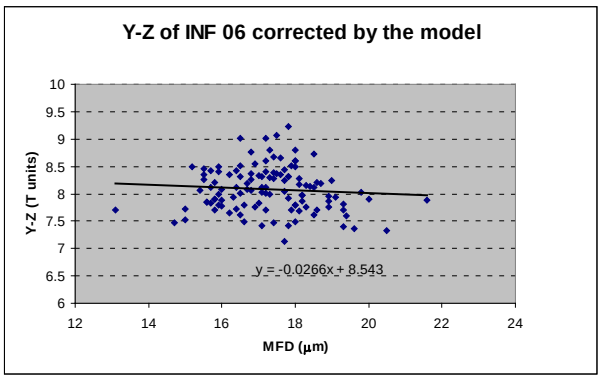

(b) Y-Z (after)

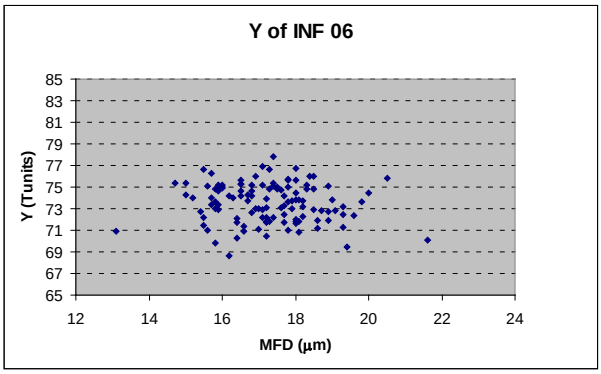

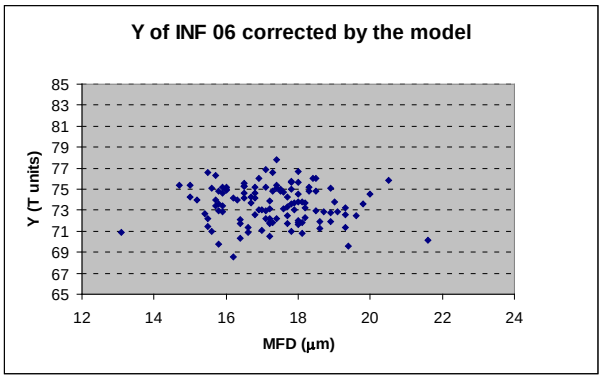

(c) Y (before) (d) Y (after)

Figure 17. Model performance for INF 06 (Struan)

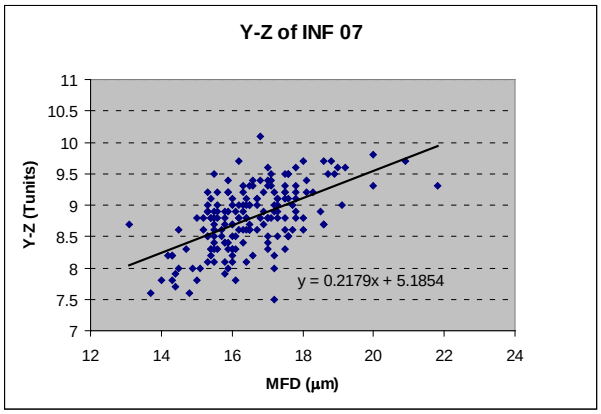

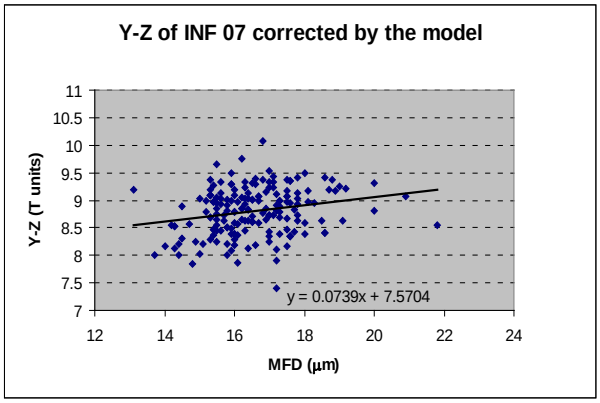

(a) Y-Z (before) (b) Y-Z (after)

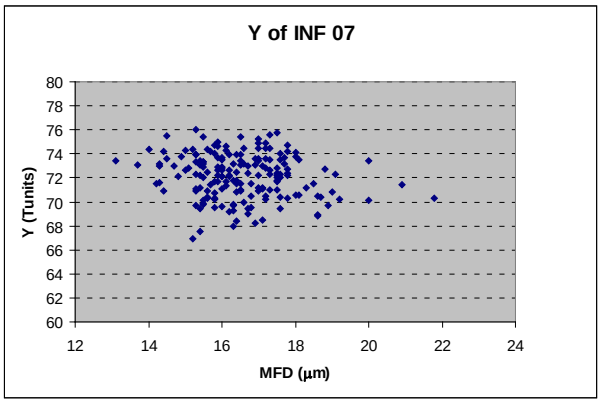

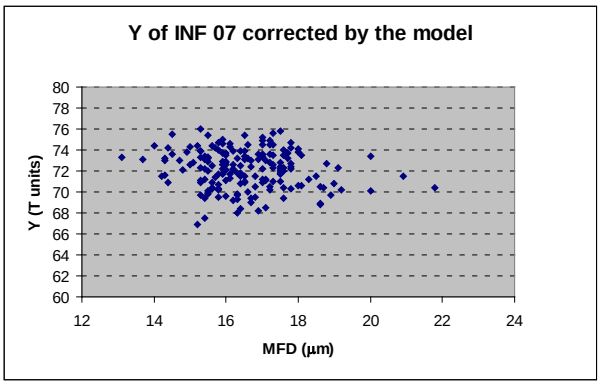

(c) Y (before) (d) Y (after)

Figure 18. Model performance for INF 07 (Turretfield)

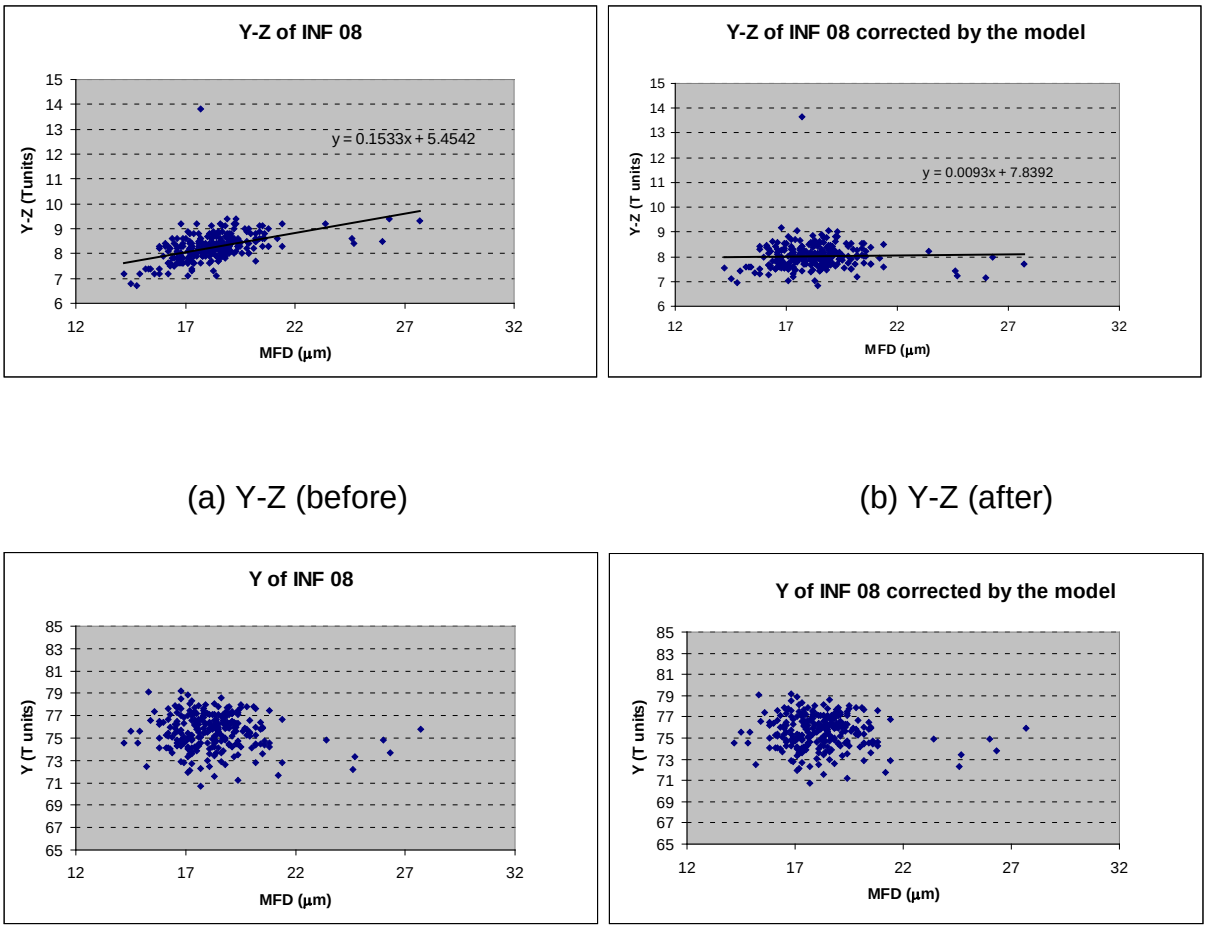

(a) Y-Z (before) (b) Y-Z (after)

(c) Y (before) (d) Y (after)

Figure 19. Model performance for INF 08 (Katanning)

Table 10. Correlation coefficients between MFD and colour values for INF's

Correction	*Colour (T units)*	MFD (micron)						
		INF01	INF03	INF04	INF05	INF06	INF07	INF08
Before	X	-0.117	-0.230	-0.153	-0.085	-0.097	-0.169	-0.122
	Y	**-0.104**	**-0.213**	**-0.134**	**-0.081**	**-0.089**	**-0.149**	**-0.109**
	Z	-0.230	-0.313	-0.275	-0.280	-0.175	-0.280	-0.243
	Y-Z	**0.451**	**0.411**	**0.500**	**0.611**	**0.360**	**0.563**	**0.442**
After	X	-0.098	-0.202	-0.129	-0.065	-0.080	-0.153	-0.097
	Y	**-0.092**	**-0.195**	**-0.119**	**-0.069**	**-0.078**	**-0.140**	**-0.094**
	Z	-0.118	-0.180	-0.134	-0.163	-0.059	-0.181	-0.093
	Y-Z	**0.138**	**0.112**	**0.095**	**0.338**	**-0.087**	**0.225**	**0.030**
Difference	X	0.02	0.03	0.02	0.02	0.02	0.02	0.03
	Y	**0.01**	**0.02**	**0.01**	**0.01**	**0.01**	**0.01**	**0.02**
	Z	0.11	0.13	0.14	0.12	0.12	0.10	0.15
	Y-Z	**-0.31**	**-0.30**	**-0.41**	**-0.27**	**-0.45**	**-0.34**	**-0.41**

Table 11. Slopes of the regression between (Y-Z) and MFD values for INF's

INF	Range of MFD μm	MFD μm	Slope before and after correction	
			Before	After
INF 01	12.9-20.3	16.2	0.199	0.055
INF 03	15.3-22.4	18.2	0.192	0.048
INF 04	13.8-19.7	16.8	0.173	0.029
INF 05	12.5-18.8	15.4	0.269	0.125
INF 06	13.1-21.6	17.3	0.117	-0.027
INF 07	13.1-21.8	16.5	0.218	0.074
INF 08	14.2-27.7	18.2	0.153	0.009

4 Implications

The results of this study could be applied to assist the CRC Wool Program achieve its goal of whiter, lightfast wool. In particular, the impact of the new correction on the genetic parameter estimates for clean colour could be explored. This could take the form of a 'before' and 'after' parameter estimation study. One would expect that if diameter covariance is removed, that this will change the phenotypic and genotypic correlations between colour and the other traits measured in CRC.
An uncorrected MFD bias would probably produce an apparent increase in wool yellowness with age. If appropriate serial colour records exist in research flocks, these could be corrected to examine the implications for lifetime values.
It would seem appropriate that SNP association analyses be conducted using the corrected colour values.
For future INF ram selection purposes, it would be very useful to conduct sire analyses using the corrected data, so that the performance of the sires to date could be evaluated.

5 Conclusions

The reflectance spectra of fibres measured by the current 'standard' method includes information about light absorption by the colorants within the fibre and about light scattering from the fibre surface and within the fibre. Fibre diameter, diameter related packing density and the thickness of the sample bulk in the measurement cell are assumed to be the major influences on this light scattering.

The Extended Multiplicative Signal Correction (EMSC) technique has been successfully applied to measurement of the clean colour of wool midside samples to quantify the effect of fibre diameter on measured wool colour, especially Wool Yellowness (Y-Z). Based on EMSC for selected samples drawn from the Kirby flock of the INF a simple-to-apply correction has been developed to remove the diameter-dependent light scattering in 'standard' colour testing of midside samples of clean wool. The correction was validated on the seven (7) INF's and was shown to reduce the dependence of (Y-Z) on MFD significantly in all cases and to reduce the dependence to approximately zero in 5 of the 7 flocks.

6 Recommendations

The models have been developed based on the assumptions established in this report. These conditions should be justified before using the models.

The models have been validated for the midside samples of the Sheep CRC 2008-2009 season INF's. The range of MFD is from 12.5μm-27.7μm. It may be worthwhile extending this modelling work to other wool samples if there is sufficient interest.

After the model corrections, INF 05 still showed a relatively strong relationship between (Y-Z) and MFD. Examination is recommended of the variation in chromophores and chromophore distribution across the diameter range for INF05. The extremes of (Y-Z) at both coarse and fine MFD's are recommended starting points for any such examination.

7 Acknowledgements

Many thanks from the authors are due to the Australian Cooperative Research Centre for funding this project. We express our sincere thanks to Dr Paul Swan for his initial input and for his advice in the implications section of this report, Dr Keith Millington of CSIRO Materials Science and Engineering for his valuable advice and support, also to Prof. Xungai Wang and Dr. Xin Liu of Deakin University for producing polypropylene filaments.

8 References

BILLMEYER, F. W. & SALTZMAN, M. (1966) *Principle of Color Technology,* NY, USA, John Wiley & Sons, Inc.

COZZOLINO, D., MONTOSSI, F. & JULIAN, R. S. (2005) The Use of Visible (VIS) and Near Infrared (NIR) Reflectance Spectroscopy to Predict Fibre Diameter in Both Clean and Greasy Wool Samples. *Animal Science,* 80**,** 333-337.

DAHM, D. & DAHM, K. (2007) *Interpreting Diffuse Reflectance and Transmittance,* Chichester, UK, NIR Publications.

FLEET, M. R., MILLINGTON, K. R., SMITH, D. H. & GRIMSON, R. J. (2009) Association of Fibre Diameter with Wool Colour in a South Australian Selection Flock *Association for the Advancement of Animal Breeding and Genetics (AAABG) 30th Anniversary Conference.* Barossa Valley, Australia.

HAMMERSLEY, M. J. & TOWNSEND, P. E. (2008) NIR Analysis of Wool. IN BURNS, D. A. & CIURCZAK, E. W. (Eds.) *Handbook of Near-Infrared Analysis.* NY, USA, CRC Press.

IWTO (2007) Method for the Measurement of Colour of Raw Wool. International Wool Textile Organisation.

KESSLER, W., OELKRUG, D. & KESSLER, R. (2009) Using Scattering and Absorption Spectra as MCR-hard Model Constraints for Diffuse Reflectance Measurements of Tablets. *Analytica Chimica Acta,* 642**,** 127-134.

KUBELKA, P. & MUNK, F. (1931) Ein Beitrag zur Optik der Farbanstriche. *Z. tech. Physik,* 12**,** 593-601.

MAHAR, T. (2007) Colour Data Analysis. Australian Wool Testing Authority Ltd.

MARTENS, H., NIELSEN, J. P. & ENGELSEN, S. B. (2003) Light Scattering and Light Absorbance Separated by Extended Multiplicative Signal Correction. Application

to Near-Infrared Transmission Analysis of Powder Mixtures. *Analytical Chemistry,* 75**,** 394-404.

STARK, E. & MARTENS, H. (1996) Multiplicative Signal Correction Method and Apparatus. US.

STARK, E. & MARTENS, H. (1997) Improved Multiplicative Signal Correction Method and Apparatus. Europe.

TILLEY, R. (2000) *Colour and Optical Properties of Materials,* London, England, John Wiley & Sons, Ltd.

WANG, H. & MAHAR, T. (2008) Correlation Analysis of Fibre Diameter and Colour of Clean Wool. Australian Wool Testing Authority Ltd.